ORIGINAL RESEARCH

Apparent Diffusion Coefficient Reveals Gray and White Matter Disease, and T2 Mapping Detects White Matter Disease in the Brain in Feline Alpha-Mannosidosis

C.H. Vite
S. Magnitsky
D. Aleman
P. O'Donnell
K. Cullen
W. Ding
S. Pickup
J.H. Wolfe
H. Poptani

BACKGROUND AND PURPOSE: Methods to locate and identify brain pathology are critical for monitoring disease progression and for evaluating the efficacy of therapeutic intervention. The purpose of this study was to detect cell swelling, abnormal myelin, and astrogliosis in the feline model of the lysosomal storage disease α-mannosidosis (AMD) by using diffusion and T2 mapping.

MATERIALS AND METHODS: Average apparent diffusion coefficient (ADC_{av}) and T2 were measured by imaging the brains of five 16-week-old cats with feline AMD on a 4.7T magnet. ADC_{av} and T2 data from affected cats were compared with data from age-matched normal cats. Brains were collected from both affected and normal cats following imaging, and histology was compared with quantitative imaging data.

RESULTS: Gray matter from AMD cats demonstrated a 13%–15% decrease in ADC_{av} compared with that in normal cats. White matter from AMD cats exhibited an 11%–16% decrease in ADC_{av} and a 5%–12% increase in T2 values compared with those in normal control cats. Histologic evidence of neuronal and glial swelling, abnormal myelin, and astrogliosis was consistent with changes in ADC_{av} and T2.

CONCLUSION: ADC_{av} and T2 data can be used to quantify differences in the gray and white matter in the feline AMD brain and may serve as surrogate markers of neuronal swelling, abnormal myelin, and astrogliosis associated with this disease. These studies may be helpful in assessing the efficacy of experimental therapies for central nervous system disease associated with lysosomal storage diseases.

Alpha-mannosidosis (AMD) is a lysosomal storage disease characterized by a deficiency of the lysosomal hydrolase acidic α-mannosidase (α-D-mannoside mannohydrolase, EC 3.2.1.24) resulting in the intralysosomal accumulation of mannose-rich oligosaccharides.[1] The disease phenotype consists of mild-to-severe psychomotor retardation with variable degrees of dysostosis multiplex, hepatosplenomegaly, ocular impairment, and hearing loss.[2] Naturally occurring AMD has also been described in cattle, cats, and guinea pigs, and a knockout mouse has been created.[3-10] AMD cats have essentially the same clinical, biochemical, and neuropathologic abnormalities as human patients[11] and have a severe clinical phenotype with grossly obvious neurologic signs, a generally uniform disease course, and death by 6 months without treatment.[12] The feline model has proved to be useful in the evaluation of experimental therapies including bone marrow transplantation and gene therapy.[13,14]

Central nervous system (CNS) pathology in both human and feline AMD includes the accumulation of oligosaccharides within cells and the resultant swelling of neurons and glia. Myelin deficiency is found, though the mechanism for the deficiency has not been identified. A diffuse astrogliosis of both gray and white matter is also described.[1,5-7,12,15,16] MR imaging methods have been used to identify surrogate markers of gray and white matter disease in feline AMD. The magnetization transfer ratio (MTR) is sensitive for detecting white matter abnormalities in multiple sclerosis and leukodystrophies.[17-19] Previous studies have shown that the MTR could be used to monitor abnormal myelination in AMD cats and improvement in myelination following successful gene therapy.[12,14] However, magnetization transfer imaging was unable to detect significant differences in gray matter between affected and normal cats.[12] Magnetization transfer imaging may also have limited application due to associated high radio-frequency power deposition, which can lead to excessive tissue heating, which can be unacceptable from an MR imaging–safety standpoint.[20] In contrast, T2 mapping is a robust, easy, and safe method, and we hypothesized that myelination abnormalities would be detected by using this technique. For imaging the disease in gray matter, we hypothesized that the average apparent diffusion coefficient (ADC_{av}) might be used to detect cell swelling and gliosis through their effect on reducing the extracellular volume fraction.[21,22] Noninvasive methods to quantify gray and white matter disease in the AMD cat

Received March 12, 2007; accepted after revision June 21.

From the W.F. Goodman Center for Comparative Medical Genetics (C.H.V., D.A., P.O., K.C., W.D.), School of Veterinary Medicine, University of Pennsylvania, Philadelphia, Pa; Department of Radiology (S.M., S.P., H.P.), School of Medicine, University of Pennsylvania, Philadelphia, Pa; and Stokes Institute (J.H.W.), Children's Hospital of Philadelphia, Philadelphia, Pa.

This work was supported by the National Institute of Neurological Disorders and Stroke (K08NS02032, C.H.V.; NS-38690, J.H.W.); National Institute of Diabetes and Digestive and Kidney Diseases (DK-63973, J.H.W.); Ara Parseghian Medical Research Foundation (C.H.V.); and a Center Grant from the National Center for Research Resources (RR-02512).

Previously presented in part at: Scientific Meeting of the International Society for Magnetic Resonance in Medicine, May 7–13, 2005; Miami, Fla; and Annual Meeting of the American Society of Gene Therapy, May 31–June 4, 2006; Baltimore, Md.

Please address correspondence to Charles H. Vite, DVM, PhD, Section of Neurology, Department of Clinical Studies, School of Veterinary Medicine, University of Pennsylvania, 3850 Spruce St, Philadelphia, PA 19105; e-mail: vite@vet.upenn.edu/

DOI 10.3174/ajnr.A0791

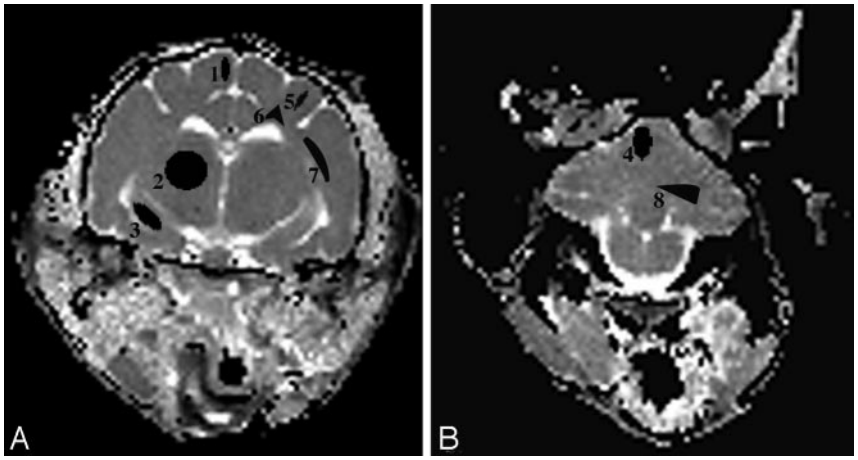

Fig 1. *A* and *B*, ADC_{av} maps of the brain at the level of the thalamus (*A*) and the cerebellum (*B*) are shown. The brain regions for which data were acquired include 4 gray matter regions (1 indicates cerebral cortex; 2, thalamus; 3, hippocampus; 4, cerebellar gray matter) and 4 white matter regions (5 indicates corona radiata; 6, centrum semiovale; 7, internal capsule; 8, cerebellar white matter).

brain should be useful for the future assessment of efficacy of experimental therapies.

Methods

Cats were raised in the animal colony under the National Institutes of Health and US Department of Agriculture guidelines for the care and use of animals in research. Five normal cats and 5 cats with AMD were examined. Peripheral blood leukocytes were tested at 1 day of age for the 4-base-pair deletion causing AMD, by using described methods.[23] All affected cats were homozygous for the mutation, and all normal cats were null for the mutation. Cats were sedated with intravenous ketamine (2.2 mg/kg) and acepromazine maleate (0.1 mg/kg) and were given intravenous atropine sulfate (0.02 mg/kg). Following sedation, cats were anesthetized with intravenous propofol (up to 6 mg/kg), intubated, and maintained under anesthesia with isoflurane for imaging experiments.

Image Acquisition and Analysis

MR images were acquired on anesthetized cats at 16 weeks of age on a 4.7T magnet (Varian, Palo Alto, Calif) equipped with 12-cm, 25-G/cm gradients. The scanner was interfaced to an Inova console (Varian), and data were acquired by using a 10-cm ID Litz coil (Doty Scientific, Columbia, SC). Core body temperature and electrocardiogram were monitored during data collection by using an MR imaging–compatible vital signs monitoring unit (Model 25; SA Instruments, Stony Brook, NY). The body temperature was maintained at 37°C by blowing regulated warm air through the magnet bore. The warm air source was supplemented with a pad with circulating heated water.

T2 maps were generated by using a multisection spin-echo protocol[24] with 4 TEs (TE = 15, 35, 55, and 75 ms). Other sequence parameters were TR = 2.5 ms, FOV = 8.0 cm^2, section thickness = 3 mm, matrix size = 128 × 128, and number of acquisitions = 1, with a total acquisition time of 25 minutes.

A spin-echo multisection diffusion-weighted imaging sequence that generates trace diffusion-tensor weighting in a single shot was used to generate ADC_{av} maps of the brain.[25] Two axial images were acquired, centered over the thalamus and the cerebellum. To minimize motion artifacts, we acquired images with cardiac gating. Diffusion-weighted images were acquired by using 5 b-values (0; 1038.6; 44,538.5; 93,461.6; and 166,154 s/cm^2). Other imaging parameters used were TR = 2 seconds, TE = 65 ms, FOV = 8.0 cm^2, section thickness = 3 mm, matrix size = 128 × 128, number of acquisitions = 1, diffusion time (Δ) = 7 ms, and duration of diffusion gradient (δ) = 5 ms. Total acquisition time was approximately 25 minutes.

The T2 and ADC_{av} maps were computed by using a nonlinear least-squares analysis in the Image Browser software (Varian) running on a computer (Sun Microsystems, Santa Clara, Calif).

Regions of interest were manually outlined with the size of the region of interest for each brain region represented as in Fig 1. Each region of interest was outlined in triplicate by 1 evaluator for each side of the brain, and the average of these measures for both sides of the brain was determined.

Histopathology

Cats were sacrificed within a week after imaging experiments by using an intravenous overdose of barbiturates in accordance with the American Veterinary Medical Association guidelines. Immediately before death, 0.5 mL of heparin (1000 U/mL) was administered intravenously. Following death, intracardiac perfusion with 250 mL of 0.9% cold saline was followed by 750 mL of universal fixative (37% formaldehyde aqueous solution; 100-mL 100% formalin, 880-mL distilled water, 2.7-g sodium hydroxide, 11.6-g sodium phosphate, and 20-mL 50% glutaraldehyde). The brain was removed and paraffin-embedded. Brain sections were stained with either hematoxylin-eosin (H&E) or Luxol fast blue. Immunohistochemistry for human glial fibrillary acidic protein (GFAP) was also performed for qualitative assessment of astrocyte numbers and astrocytic processes (astrogliosis).

Measurements of Purkinje cell area were performed manually by acquiring digital photos of ×400 sections of the cerebellar cortex of 5 AMD and 5 normal cats. Images were opened with Photoshop (Adobe Systems, San Jose, Calif), and the area of 40 Purkinje cells per cat in which the nucleus was readily visible was determined. Area measurements were made by tracing the cytoplasmic border of each cell by using the magnetic lasso tool and by using the histogram option to provide the mean number of pixels within the area traced.

Statistical Methods

Mean and SD were used to describe region of interest and area data. An unpaired 2-tailed *t* test was used to compare mean T2, ADC_{av}, and area data between affected and normal cats. A value of $P < .05$ was considered significant.

Results

All animals tolerated the imaging session well. Representative ADC_{av} maps are shown in Fig 1. Four gray matter structures (cerebral cortex, thalamus, hippocampus, and cerebellar gray matter) and 4 white matter regions (corona radiata, centrum semiovale, internal capsule, and cerebellar white matter) were examined in both the left and right sides of the brain as in the previous study.[12]

Significant increases in T2 were found in the white matter

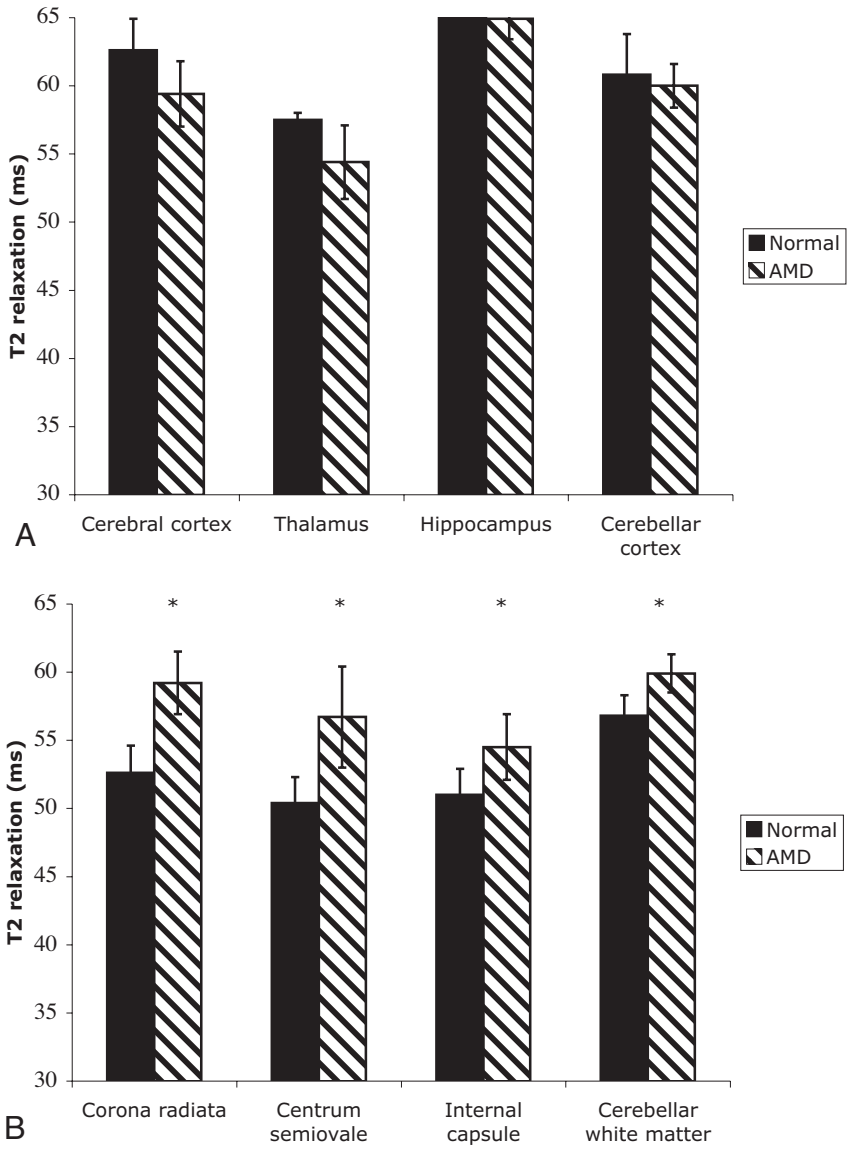

Fig 2. T2 relaxation times of gray matter regions (cerebral cortex, thalamus, hippocampus, and cerebellar cortex and white matter regions (corona radiata, centrum semiovale, internal capsule, and cerebellar white matter [bottom]) were determined in unaffected and AMD cats. Significant increases in T2 were found in the white matter of AMD cats compared with unaffected cats (*$P < .05$). No significant differences in T2 were found between affected and normal cats when gray matter regions were compared.

of affected cats compared with unaffected cats in all white matter regions examined (Fig 2). The T2 of the white matter was 5%–12% higher than that found in unaffected cats in these white matter regions, with the greatest increases in T2 found in the corona radiata and centrum semiovale. In contrast, no significant differences in T2 were found in the gray matter of affected cats, compared with unaffected cats.

Significant decreases in ADC_{av} were found in both the gray and white matter of affected cats, compared with unaffected cats in all brain regions examined (Fig 3). In AMD cats compared with unaffected cats, the decrease in ADC_{av} in the gray matter was 13%–15% and the decrease in ADC_{av} in the white matter was 11%–16%.

Microscopic evaluation of H&E-stained sections from affected cats showed cytoplasmic vacuolation and distention of neurons, glia, and endothelial cells in the gray matter (Fig 4*B*). We compared the distention of the Purkinje cells in AMD and normal cats. Purkinje cell bodies of AMD cats occupied a mean of 15,501 ± 2947 pixels, and cell bodies from normal cats had a mean of 10,847 ± 2367 pixels. A statistically significant difference was found between AMD and normal cats in these measurements ($P = .04$). Cytoplasmic vacuolation and distended glial cells were also seen in the white matter of AMD cats. H&E-stained sections and Luxol fast blue–stained sections showed a decrease in myelin, evidenced by decreased Luxol fast blue staining and distension and splitting of the myelin sheaths as has been reported previously (Fig 4*D*).[12] A diffuse astrogliosis was present throughout the gray and white matter as seen by an increase in GFAP-positive cells and their processes. This reactive, proliferative astrogliosis occurred in the absence of significant neuronal death (Fig 4*F*). Cytoplasmic vacuolation, abnormal myelin, and astrogliosis were diffusely present throughout the brain, with no evidence of regional differences.

Discussion

Lysosomal storage diseases are characterized by the deficiency of specific lysosomal hydrolases, resulting in severe degenerative processes affecting a number of tissues, including the brain.[26] More than 45 lysosomal storage diseases have been identified, and whereas the prevalence of each lysosomal storage disease is rare, together this family of disorders affects approximately 1 in 5000 humans,[27,28] making them a clinically significant set of genetic disorders. Effective therapy for CNS disease in most of these disorders remains to be developed. Animal models of lysosomal storage diseases have proved to be critical for evaluating treatment strategies for lysosomal storage disease,[29,30] and noninvasive methods are necessary to monitor the efficacy of experimental therapies on CNS pathology.[31]

CNS pathology in feline AMD includes cellular swelling, decreased myelin, and astrogliosis.[5-7,12] It has been reported that AMD cats imaged at 1.5T have significant decreases in the magnetization transfer ratio (MTR) of white matter compared with normal cats,[12] whereas the MTRs were increased in cats treated with gene therapy,[14] providing evidence that MTR could be used to monitor improvements in myelination associated with therapy. These studies showed that MTR was a useful noninvasive antemortem method to quantify myelin deficiency subsequently confirmed postmortem.[12] In the present study, we evaluated the T2 relaxation times of the white and gray matter in AMD cats as an alternative MR imaging parameter because T2 measurements are standard, may

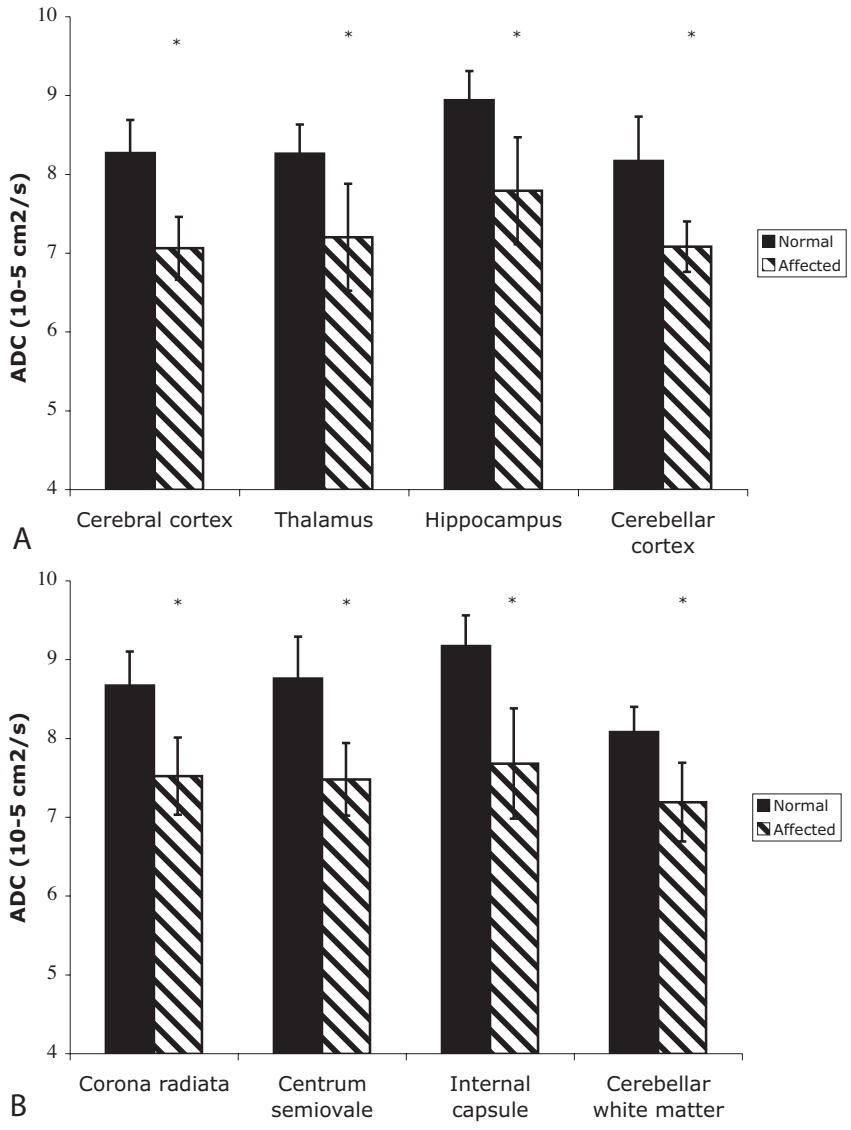

Fig 3. ADC_{av} of gray matter regions (cerebral cortex, thalamus, hippocampus, and cerebellar cortex and white matter regions (corona radiata, centrum semiovale, internal capsule, and cerebellar white matter [bottom]) were determined in unaffected and AMD cats. Significant decreases in ADV_{av} were found in AMD cats in all gray and white matter regions examined ($^*P < .05$).

be readily performed, and do not result in high-energy absorption associated with MT imaging. Significant increases in T2 were found in the corona radiata, centrum semiovale, internal capsule, and cerebellar white matter of AMD cats compared with normal cats, with the increases being found in the same tracts as the decreases in MTR in the previously reported study.[12] The increase in T2 of the white matter is probably due to the reduced myelin found in AMD cats compared with control cats. Additionally, astrogliosis present in diseased cats may also contribute to the increase in T2. As with the previous MTR studies, which were performed at 1.5T, T2 measurements could not distinguish changes in the gray matter of AMD cats compared with normal cats. The effect of intracellular oligosaccharide accumulation on T2 relaxation times has not yet been determined. However, the most obvious cell swelling occurs in the neuron cell bodies of the gray matter regions, where we did not observe any difference in T2 relaxation times between affected cats and normal cats, suggesting that oligosaccharide accumulation may not affect the T2 values significantly.

One goal of our study was to identify a marker of gray matter disease (cell swelling and astrogliosis). Diffusion-weighted imaging can noninvasively quantify water molecule random motion that is sensitive to pathologic changes in tissues.[32] Although the exact mechanism responsible for reduction in ADC following cellular swelling is not well understood, reduction in ADC correlates with reduction in the extracellular volume fraction.[22] In stroke, ischemia results in cell swelling by cytotoxic edema, and ADC of brain water declines.[33] As cell swelling associated with ischemia resolves, an increase in the diffusion coefficient of water has been described.[34] Similar correlations between reductions in ADC and cellular swelling are described following toxin administration,[35] status epilepticus,[36] cortical spreading depression,[37] and hypoglycemia.[38] Diffusion imaging has thus far not been used to evaluate cell swelling in any lysosomal storage disease. We hypothesized that the swelling of neurons and glia associated with the storage of oligosaccharides as well as an increase in astrocyte number and their processes (astrogliosis) would decrease the extracellular volume leading to a decrease in ADC_{av} of the gray matter. We observed significant decreases in ADC_{av} in the gray matter of cats with AMD compared with normal cats but were not able to determine whether this decrease was due to cell swelling alone or also due to astrogliosis because both are diffusely present in the AMD brain.

We also hypothesized that the abnormal myelin would result in decreases in ADC_{av} of the white matter as has been described in Canavan disease and metachromatic leukodystrophy.[39-41] In these leukodystrophies, the decrease in ADC was attributed to restriction of water diffusion due to myelin breakdown and to a general increase in lysosomal membranes and macromolecules.[39-41] In Canavan disease, astrogliosis and electron microscopic evidence of separation of myelin layers with intramyelinic vacuole formation were also proposed to lower ADC values.[39] Histologic evaluation of the white matter of AMD cats shows decreased myelination with splitting of myelin sheaths, as well as severe astrogliosis, both of which could restrict water diffusion. Because electron microscopic evaluation of feline brain tissue was not performed in this study, we cannot comment on the white matter ultrastructure. Additionally, unlike Canavan disease and metachromatic leukodystrophy, swelling of glia is also a feature of AMD and

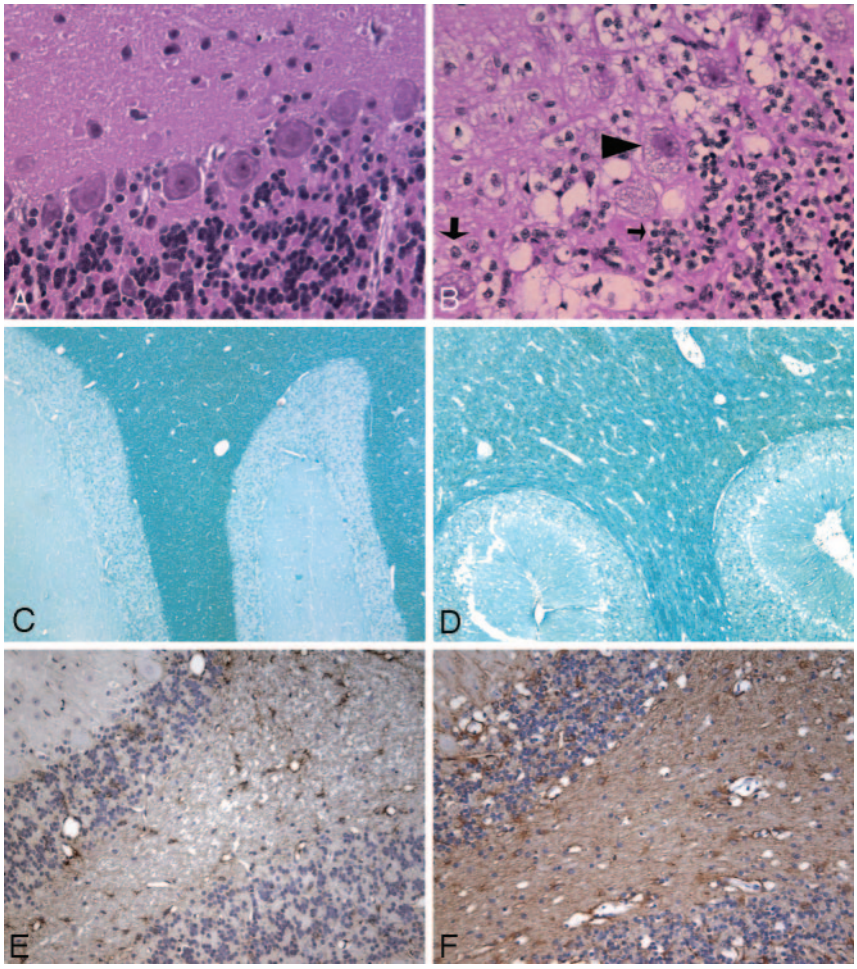

Fig 4. *A* and *B*, H&E-stained sections of the cerebellar cortex (original magnification ×400) from a normal cat (*A*) and an AMD cat (*B*), showing cytoplasmic vacuolation and distention of Purkinje cells (*arrowhead*), granular cells (*small arrow*), and glia (*large arrow*). *C* and *D*, Luxol fast blue staining of the cerebellar white matter (original magnification ×50) from a normal cat (*C*) and an AMD cat (*D*). A decrease in myelination is seen as a decrease in stain intensity and as an increase in space between myelin sheaths. *E* and *F*, GFAP immunohistochemistry of the cerebellum (original magnification ×200) from a normal (*E*) and an AMD cat (*F*), showing diffuse astrogliosis (brown staining) present throughout the gray and white matter of affected cats.

could have contributed to decreased water diffusion in the extracellular space. We were unable to determine the specific contribution of myelin breakdown, cell swelling, and astrogliosis to the decrease in ADC found in the white matter.

Although widely available, measurement of ADC_{av} is not trivial because the ADC_{av} values are highly sensitive to motion and temperature variability, which was effectively dealt with in these studies through the use of anesthesia, cardiac gating, and maintenance of body temperature. A second limitation to ADC_{av} measurements is the assumption that decreased water diffusion in the extracellular space makes the most significant contribution to decreases in ADC_{av} measurements, even though water diffusion in the intracellular compartment also contributes to its ADC_{av} measurements.[21] Finally, as stated previously, cell swelling, astrogliosis, and/or myelin abnormalities all can contribute to a reduction in the extracellular volume; thus, the exact histopathologic correlate of the decrease in ADC_{av} could not be determined. To identify a surrogate marker of cell swelling alone, one would have to use other nuclear MR methods, such as diffusion-weighted MR spectroscopy.

There are little data from patients that can be directly compared with data collected from AMD cats. In human patients, a severe infantile form and a milder adult form of AMD are described.[2] Affected cats have a rapid progression of severe clinical signs, which results in death by 6 months of age, making the disease in cats more similar to the infantile form. To our knowledge, MR imaging data have been published on only 3 patients with the infantile form.[42] The authors describe changes in the periventricular white matter including prominent Virchow-Robin spaces and T2 hyperintensity. Diffusion studies were not done in these patients.

In the cats, diffusion images were acquired in approximately 25 minutes. Although the methods used would be long for clinical translation, most clinical diffusion studies are performed by using an echo-planar imaging (EPI) sequence, which may be completed within a few minutes without gating. EPI-based diffusion studies were not performed in these cats because the artifacts due to the susceptibility-induced effects at higher fields (4.7T) are much greater. It is possible that ADC_{av} measurements could be useful in assessing patients with AMD, provided that lower b-values are used. Because a single monoexponential fit was performed for the diffusion analysis, smaller b-values, available on clinical scanners, should lead to similar findings without compromising the signal intensity-to-noise ratio (SNR). The use of multireceiver phased-array coils, available on many clinical scanners, may also improve SNR and/or reduce acquisition time. Finally, the larger size of the human brain compared with the cat brain may not require images with a resolution as high as were generated in these cat studies, thus further increasing SNR.

Conclusion

ADC_{av} and T2 data can be used to quantify differences in the gray and white matter in the feline AMD brain and may serve as surrogate markers of neuronal swelling, abnormal myelin, and astrogliosis associated with this disease. These data may be used to assess the efficacy of experimental therapies for CNS disease associated with lysosomal storage diseases.

Acknowledgments

All MR imaging studies reported in the current manuscript were performed at the Small Animal Imaging Facility in the Department of Radiology at the University of Pennsylvania.

References

1. Ockerman PA. **A generalized disorder resembling Hurler's syndrome.** *Lancet* 1967;i:239–41
2. Thomas G. **Disorders of glycoprotein degradation: α-mannosidosis, β-mannosidosis, fucosidosis, and sialidosis.** In: Scriver CR, Valle D, Sly WS, eds. *The Metabolic and Molecular Bases of Inherited Disease.* New York: McGraw Hill; 2001:3507–34
3. Hocking JD, Jolly RD, Batt RD. **Deficiency of alpha-mannosidase in Angus cattle: an inherited lysosomal storage disease.** *Biochem J* 1972;128:69–78
4. Burditt LJ, Chotai K, Hirani S, et al. **Biochemical studies on a case of feline mannosidosis.** *Biochem J* 1980;189:467–73
5. Vandevelde M, Fankhauser R, Bichsel P, et al. **Hereditary neurovisceral mannosidosis associated with alpha-mannosidase deficiency in a family of Persian cats.** *Acta Neuropathol (Berl)* 1982;58:64–68
6. Jezyk PF, Haskins ME, Newman LR. **Alpha-mannosidosis in a Persian cat.** *J Am Vet Med Assoc* 1986;189:1483–85
7. Maenhout T, Kint JA, Dacremont G, et al. **Mannosidosis in a litter of Persian cats.** *Vet Rec* 1988;122:351–54
8. Cummings JF, Wood PA, de Lahunta A, et al. **The clinical and pathologic heterogeneity of feline alpha-mannosidosis.** *J Vet Intern Med* 1988;2:163–70
9. Crawley AC, Jones MZ, Bonning LE, et al. **Alpha-mannosidosis in the guinea pig: a new animal model for lysosomal storage disorders.** *Pediatr Res* 1999;46:501–09
10. Stinchi S, Lullmann-Rauch R, Hartmann D, et al. **Targeted disruption of the lysosomal alpha-mannosidase gene results in mice resembling a mild form of human alpha-mannosidosis.** *Hum Mol Genet* 1999;8:1365–72
11. Sun H, Wolfe JH. **Recent progress in lysosomal alpha-mannosidase and its deficiency.** *Exp Mol Med* 2001;33:1–7
12. Vite CH, McGowan JC, Braund KG, et al. **Histopathology, electrodiagnostic testing, and magnetic resonance imaging show significant peripheral and central nervous system myelin abnormalities in the cat model of alpha-mannosidosis.** *J Neuropathol Exp Neurol* 2001;60:817–28
13. Walkley SU, Thrall MA, Dobrenis K, et al. **Bone marrow transplantation corrects the enzyme defect in neurons of the central nervous system in a lysosomal storage disease.** *Proc Natl Acad Sci U S A* 1994;91:2970–74
14. Vite CH, McGowan JC, Niogi S, et al. **Effective gene therapy for an inherited diffuse CNS disease in a large animal model.** *Ann Neurol* 2005;57:355–64
15. Kjellman B, Gamstorp I, Brun, et al. **Mannosidosis: a clinical and histopathologic study.** *J Pediatr* 1969;75:366–73
16. Lake BD. **Lysosomal and peroxisomal disorders.** In: Adams, JH, Duchen LW, eds. *Greenfield's Neuropathology*. New York: Oxford University Press; 1997:706–07
17. Dousset V, Grossman RI, Ramer KN, et al. **Experimental allergic encephalomyelitis and multiple sclerosis: lesion characterization with magnetization transfer imaging.** *Radiology* 1992;182:483–91
18. Brochet B, Dousset V. **Pathological correlates of magnetization transfer imaging abnormalities in animal models and humans with multiple sclerosis.** *Neurology* 1999;53:S12–17
19. Back T, Mockel R, Hirsch JG, et al. **Combined MR measurements of magnetization transfer, tissue diffusion and proton spectroscopy: a feasibility study with neurological cases.** *Neurol Res* 2003;25:292–300
20. Finelli DA, Rezai AR, Ruggieri PM, et al. **MR imaging-related heating in deep brain stimulation electrodes: in vitro study.** *AJNR Am J Neuroradiol* 2002;23:1795–802
21. Gass A, Niendrof T, Hirsch JG. **Acute and chronic changes of the apparent diffusion coefficient in neurological disorders: biophysical mechanisms and possible underlying histopathology.** *J Neurol Sci* 2001;186:S15–23
22. Sotak CH. **Nuclear magnetic resonance (NMR) measurement of the apparent diffusion coefficient (ADC) of tissue water and its relationship to cell volume changes in pathological states.** *Neurochem Int* 2004;45:569–82
23. Berg T, Tollersrud OK, Walkley SU, et al. **Purification of feline lysosomal alpha-mannosidase, determination of its cDNA sequence and identification of a mutation causing alpha-mannosidosis in Persian cats.** *Biochem J* 1997;328:863–70
24. Jezzard P, Duewell S, Balaban RS. **MR relaxation times in human brain: measurement at 4 T.** *Radiology* 1996;199:773–79
25. Mori S, van Zijl PC. **Diffusion weighting by the trace of the diffusion tensor within a single scan.** *Magn Reson Med* 1995;33:41–52
26. Scriver CR, Beaudet AL, Sly WS, et al. *Metabolic Bases of Inherited Disease,* 8th ed. New York: McGraw Hill: 2001; 3369–94
27. Meikle PJ, Hopwood JJ, Clague AE, et al. **Prevalance of lysosomal storage disorders.** *JAMA* 1999;281:249–54
28. Beaudet AL, Scriver CR, Sly WS, et al. **Genetics, biochemistry and molecular bases of variant human phenotypes.** In: Scriver CR, Beaudet AL, Valle D, Sly WS, eds. *The Metabolic and Molecular Bases of Inherited Disease.* New York: McGraw Hill; 2001:1–128
29. Watson DJ, Wolfe JH. **Lentiviral vectors for gene transfer to the central nervous system: applications in lysosomal storage disease animal models.** *Methods Mol Med* 2003;76:383–403
30. Ellinwood NM, Vite CH, Haskins ME. **Gene therapy for lysosomal storage diseases: the lessons and promise of animal models.** *J Gene Med* 2004;6:481–506
31. Wolfe JH, Acton P, Poptani H, et al. **Molecular imaging of gene therapy for neurogenetic diseases.** In: Kaplitt MG, During MJ, eds. *Gene Therapy in the Central Nervous System: From Bench to Bedside.* San Diego, Calif: Academic Press; 2006:335–50
32. Le Bihan D, Turner R, Doek P, et al. **Diffusion MR imaging: clinical applications.** *AJR Am J Roentgenol* 1992;159:591–99
33. Moseley ME, Cohen Y, Mintorovitch J, et al. **Early detection of regional cerebral ischemia in cats: comparison of diffusion- and T2-weighted MRI and spectroscopy.** *Magn Reson Med* 1990;14:300–46
34. Davis D, Ulatowski J, Eleff S, et al. **Rapid monitoring of changes in water diffusion coefficients during reversible ischemia in cat and rat brain.** *Magn Reson Med* 1994;231:454–60
35. Buckley DL, Bui DL, Phillips MI, et al. **The effect of ouabain on water diffusion in the rat hippocampal slice measured by high resolution NMR imaging.** *Magn Reson Med* 1999;41:137–42
36. Zhong J, Petroff OAC, Prichard JW, et al. **Changes in water diffusion and relaxation properties of rat cerebrum during status epilepticus.** *Magn Reson Med* 1993;30:241–46
37. Latour LL, Hasegawa Y, Formata JE, et al. **Spreading waves of decreased diffusion coefficient after cortical stimulation in the rat brain.** *Magn Reson Med* 1994;32:189–98
38. Hasegawa Y, Formato JE, Latour LL, et al. **Severe transient hypoglycemia causes reversible changes in the apparent diffusion coefficient of water.** *Stroke* 1996;27:1648–56
39. Engelbrecht V, Scherer A, Rassek M, et al. **Diffusion-weighted MR imaging in the brain in children: findings in the normal brain and in the brain with white matter diseases.** *Radiology* 2002;222:410–18
40. Sener RN. **Metachromatic leukodystrophy. Diffusion MR imaging and proton MR spectroscopy.** *Acta Radiol* 2003;44:440–43
41. Oguz KK, Anlar B, Senbil N, et al. **Diffusion-weighted imaging findings in juvenile metachromatic leukodystrophy.** *Neuropediatrics* 2004;35:279–82
42. Patlas M, Shapira MY, Nagler A, et al. **MRI of mannosidosis.** *Neuroradiology* 2001;43:941–43